UCRL -71316
PREPRINT

Lawrence Radiation Laboratory
UNIVERSITY OF CALIFORNIA
LIVERMORE

THE FATIGUE BEHAVIOR OF A HIGH DENSITY GRAPHITE AND A GENERAL DESIGN CORRELATION

H. Leichter
E. Robinson

August 26, 1968

This manuscript was prepared for submittal to the American Ceramic Society 71st Annual Meeting and Exposition, Washington, D. C., May 3-8, 1969.

DISCLAIMER

THE FATIGUE BEHAVIOR OF A HIGH DENSITY GRAPHITE AND A GENERAL DESIGN CORRELATION

H. Leichter and E. Robinson

Lawrence Radiation Laboratory, University of California

Livermore, California 94550

ABSTRACT

The fatigue behavior of a high-density graphite* was investigated in reverse bending up to 5×10^8 cycles at room temperature. A statistical analysis was made of fatigue life, using a Weibull distribution and a homologous stress. The homologous stress is the ratio of applied stress in fatigue to the expected first-cycle strength. The first-cycle strength was calculated from the bending tests of similar material or "mate" specimens, using the Weibull statistical strength theory for correction of the significant size effect. Homologous stress gives an essentially invariant fatigue correlation for many graphite grades and may be used for the estimation of fatigue life under a wide variety of operating conditions. The practical endurance limit for graphite was found to correspond to a homologous stress of about 47%.

INTRODUCTION

The recent interest in graphite as a material for high-temperature rotating machinery[1] has naturally raised questions concerning its fatigue behavior. Its

This work performed under the auspices of the U.S. Atomic Energy Commission.

*Grade EP-1924 graphite, a fine-grain dense graphite which is currently designated AXF. The grain size is 0.001 in. and the density is 1.88 g/cc.

highly variable strength and its brittle nature have previously discouraged applications in which the material would be subjected to alternating stresses for prolonged periods. As a result, very few data on graphite fatigue are presently available. Green,[2] in a limited number of fatigue tests on AUF graphite in reverse bending at room temperature and at 3550°F, found that the apparent endurance limit of 2500 lb/in.^{2} at room temperature increased to about 4400 lb/in.^{2} at 3550°F. This is consistent with the increased static strength with increased temperature displayed by most graphites. The 10^6-cycle fatigue strength of pyrolytic graphite has been reported to be 6500 lb/in.^{2} with a scatter band of ±2000 lb/in.^{2} at room temperature.[3] In an attempt to find the influence of proof testing on the probability of failure of CFW graphite, Dally[4] reports that low-cycle failure damage (up to 100 cycles) is cumulative, and that both the number of cycles and the stress level influence the failure probability. Some preliminary flexure fatigue data for a fiber-reinforced graphite* at room temperature were published recently by France and Kachur.[5] They report an apparent endurance limit of 32,000 lb/in.^{2} in reverse bending for this material.

Recent work in Russia by Barabanov et al.[6] on a fairly high-density molded graphite (1.78 to 1.99 g/cm^3) shows the fatigue strength in directions parallel to the transverse to the pressing axis. The difference in fatigue strength between the two orientations is in the same ratio as that of the corresponding static strengths. They also investigated the effect of gage-section geometry upon the fatigue results and found (as one would expect on the basis of current theories regarding brittle behavior) a higher average value combined with increased scatter as the effective gage section was reduced. They also

*Carbitex 715.

apparently experienced a high incidence of failure during initial load application. Their results show an approximate average fatigue life of 10^7 cycles at a homologous stress* of 65%.

In experimental studies of fatigue, the results for a brittle material, unlike those for a ductile material, are determined mainly by the high variability in strength and by the apparent dominance of the "worst-flaw" mechanism. This mechanism results in a size effect, which must be recognized for proper utilization of the data in design.

The purpose of this study was to examine the fatigue behavior of EP-1924 graphite from a statistical viewpoint, to correlate this with the homologous strength, and to develop design for high probability of survival for a variety of graphites.

SPECIMENS AND TEST PROCEDURE

The material available for testing comprised fifty 1/4-in. centerless ground EP-1924 graphite rods, all 6 in. long. The rods were coded at both ends, and a fatigue test specimen and a "mate" static test specimen were cut from each. Details of the fatigue test specimens are shown in Fig. 1. The

*Homologous stress is here defined as the ratio of applied stress in fatigue to the expected strength. The expected strength is the stress causing failure within the first cycle. The expected first-cycle strength is computed from the bending tests of similar material using the Weibull theory for size-effect correction, or estimated by a rearward extrapolation of published fatigue results to one-cycle life.

reduced section was located and sized so that the stress there would exceed the maximum stress at the drive collet by a factor of 1.5 to 2.0.

The fifty "mate" specimens were of constant diameter (1/4 in.) and were tested in three-point bending on a 10k Instron test machine equipped with a 100-lb load cell. The span used was 2-3/8 in. and the cross-head trave was 0.02 in./min (see Appendix A for the statistical analysis of "mate" strength).

The Krouse rotating-beam fatigue machine and the related equipment were calibrated as outlined in Appendix B. A few graphite fatigue specimens were sacrificed to determine the proper operating procedure. It was found, for example, that some specimens were slightly warped along the long axis. Care had to be taken when installing them in the drive collet to ensure that eccentricity was minimal both at the spindle end and at the gage section, to minimize errors in bending stress. The run-out measured with a dial indicator could usually be kept within 0 to 0.002 in.; however, it was greater in some specimens. It was found also that resonance vibrations occurred at motor speeds of about 4000 to 5000 rpm, and it was necessary to pass quickly through this region while manually damping the vibration at the spindle-bearing housing.

The bending moment to produce the desired alternating stress on a fatigue specimen was set on the machine by the use of a strain-gaged steel beam as shown in the upper part of Fig. 2. The strain setting corresponding to the desired stress was first calculated using Eq. (B-2) from Appendix B:

$$\epsilon_s = 0.01087\ \sigma_g \mu\text{in./in.} \qquad (1)$$

where ϵ_s = strain in steel beam in in./in., and σ_g = maximum fiber stress in lb/in.^{2} in the graphite at the reduced section. The approximate moment setting was found from Fig. 10, and the sliding weight was finely

adjusted on the graduated lever arm until the average of the two strain-gage readings gave the desired strain. The weight was then locked in place. Strain readings were obtained with a Datran digital readout unit. After the graphite fatigue-test specimen was properly installed in the drive and spindle collets, moment was carefully applied by removing the spindle support and slowly lowering the spindle bearing manually. The drive shaft was turned through a maximum of 50 cycles by hand. If failure had not occurred, the motor was started and allowed to turn at about 500 rpm until several thousand cycles had been accumulated on the counter. The speed was then rapidly increased to 10,000 rpm while the load was manually supported to minimize the deleterious effects of low-speed wobble and of the resonances mentioned above. At speed, the load was gradually transferred to the fatigue-test specimen again, and the machine was allowed to run until fracture occurred or until the test was otherwise terminated. The lower part of Fig. 2 shows a fatigue test in progress. When a specimen failed the spindle and the weighted lever arm dropped, closing the microswitch and thus stopping the motor.

RESULTS AND DISCUSSION

S-N diagrams for EP-1924 graphite are shown in Fig. 3 with 50%, 10% and 1% probability of failure contours. The statistical analysis for deriving these probability contours is described in detail in Appendix C. In Fig. 3a, the homologous stress is the applied stress divided by the strength of the corresponding "mate" specimen (corrected for size effect). In Fig. 3b the homologous stress is the applied stress divided by the mean strength of all "mate" specimens tested

(also corrected for size effect). The importance of the size-effect correction is discussed in Appendix A. The 50% and 10% failure probability points based on both kinds of homologous stress are plotted in Fig. 3c. The correlation is slightly better when homologous stress is based on individual "mate" strength. However, the improvement may not justify the necessary maintenance of identification between operational component and test specimen.

Because of the considerable strength variation of EP-1924, each fatigue specimen was inspected radiographically before testing. Many specimens showed indications of either low-density or high-density inclusions (or flaws) in the test section, but no meaningful correlation could be made with fatigue strength. Examination of the fracture surfaces of the specimens also revealed some rather large high-density or low-density areas (Fig. 4), but some of these specimens had longer life than specimens showing no such areas. It is quite evident, however, that even though no correlation was found, large inclusions did influence fracture: when present, they were always found opposite the compression lip, and were apparently the site of fracture initiation. Such inclusions were not always detected by radiography. It may be that such flaws characterizing this material, and that their severity in fatigue does not correspond with their visibility.

An additional factor that required resolution was the occurrence of failure within the first cycle. The stress causing such failure should be the normalizing factor used in computing the homologous stress. A specimen selected at random and intended for testing at a specific fatigue-stress level must first survive the first cycle; that is, all specimens fatigue-tested at a given stress level are certain to possess strengths exceeding the test level. Thus it is no surprise that in testing at relatively high stress, fracture sometimes occurs during the first cycle because of insufficient strength. From the Weibull

distribution with m = 9, we expect that tests at 90% of the mean first-cycle strength cause about 21% failure, while those at 67% of the mean will cause about 2% failure. It is now possible to describe quantitatively the failures occurring within the first cycle. The data tables in Appendix C show the failure probability corresponding to each fatigue level (whether expressed as homologous strength based on each "mate" or simply as the fatigue stress), and the number of static failures that would be expected. The observations are consistent with the predictions at the bottom of each data table. The correct estimate of fatigue-life probability is the product of the probability that an arbitrary specimen will have a sufficient static strength to survive the first cycle, and the probability, derived from the charts of this report, that the fatigue-specimen lifetime will then equal or exceed a specified value. For example then, a specimen under fatigue at about 60% of its expected strength (complete reversal) is expected to exceed 100 cycles with 99% probability. The chance of choosing such a specimen at random is slightly less, since the probability of static failure at this level approaches 2%.

The generalized correlation obtained with the homologous S-N diagram (as shown in Fig. 3) is superior to the conventional S-N diagram. It represents operational stress as a fraction of expected strength under the operational conditions and is free of size effect. Also, the homologous plot may be used to estimate fatigue life at any temperature, since it is based on the strength of the specimen. The increase in apparent endurance limit with temperature and strength has been demonstrated by Green[2] and Barabanov et al.[6] Such behavior is expected if this homologous stress is the correct correlation for fatigue life.

The generalized homologous stress correlation was tested for a variety of published graphite-fatigue data.[2-6] These graphites exhibited strengths ranging from about 2000 psi to about 50,000 psi. The normalized first-cycle strength for computing homologous stress was estimated by extrapolating the fatigue curve back to one cycle lifetime. All of these data including those of our experiment are plotted in Fig. 5 with the probability contours derived from our data superimposed.

As a final observation, fatigue data for metals[7] analyzed by the Weibull distribution exhibit no less variability than that observed for graphite, while the endurance limits are frequently at a lower homologous stress. An example is the apparent endurance limit for 18% nickel maraging steels, which may be as low as 37% of the ultimate tensile strength,[8] i.e., considerably less than that found for graphite.

CONCLUSIONS AND RECOMMENDATIONS

1. The fatigue behavior of EP-1924 graphite is well correlated with a homologous stress parameter based on tests of "mate" specimens and estimates of first-cycle strength. This parameter is also more convenient to use in estimating fatigue behavior under a variety of stress and temperature conditions, and is shown to give good correlation for a wide variety of published graphite-fatigue data. A homologous stress parameter should be considered in studies of all brittle materials.

2. A Weibull distribution for the analysis of strength and lifetime is preferred because it is applicable to both fatigue and fracture analysis, it is more conservative than the corresponding normal distribution, it is a fairly simple analytical form, and it is central to the study of the strength of brittle materials.

3. Visible flaws on the fracture surfaces of fatigue specimens did not seem to affect the expected fatigue life but did influence the site of fracture initiation. These flaws (or inclusions) are believed to be expected statistical extensions of the population of flaws characterizing this material.

4. The endurance limit for EP-1924 graphite is about 47% of the first-cycle strength. This interpretation is recommended as a design estimate for any stress distribution, and is probably reasonable for most graphites.

5. The conclusion that "work-hardening" can occur as a result of fatigue-testing a brittle material[9] is probably a misinterpretation of the screening process previously described. All specimens surviving fatigue at a significant fraction of their strength will necessarily be a selected sample, whose strength exceeds the population average.

ACKNOWLEDGMENTS

The authors wish to express their appreciation to T. C. Mamaros and R. Cortez, both of the Engineering Test Laboratory, Support Division (LRL), for their assistance in performing the dynamic and static tests, respectively.

APPENDIX A

ESTIMATION OF FIRST-CYCLE STRENGTHS FROM BENDING TESTS OF "MATES"

For each fatigue specimen, a "mate" was cut from the same original piece of 1/4-in.-diam blank. These "mates" were tested in three-point bending to obtain the modulus of rupture and the distribution of strength. Table 1 gives the results of two types of statistical analysis in which a Weibull distribution is fitted to the data assuming either one or three modes. The column labeled "mutlimode analysis" represents the observations grouped into three modes (which in this case were estimated by eye), with each observation in such a subgroup divided by the mode average. Each of the modes was fitted by a Weibull distribution (shown in Fig. 6 and Table 2), and the modes were then combined to give the failure probability expected of the composite population as plotted in Fig. 7. The results of this analysis show that a unimodal Weibull distribution with $m \approx 9$ gives a reasonable fit (and one consistent with other results on this material), though some refinement may be obtained by resorting to the three-mode fit (Fig. 7).

In order to properly compare the relative strengths of the "mate" in the three-point bending test and the corresponding rotating-cantilever fatigue specimen, we use the result given by Robinson[10] for the risk of rupture of a round rod in three-point bending:

$$R_B = \left(\frac{\sigma_B}{\sigma_0}\right)^m \frac{2\ell_B r_B^2}{(m+1)(m+2)} \left(\frac{\sqrt{\pi}}{2}\right) \frac{\Gamma\left(\frac{m+1}{2}\right)}{\Gamma\left(\frac{m}{2}+1\right)}$$

where R_B = risk of rupture

σ_B = stress in bend specimen

m = Weibull modulus

ℓ_B = length of bend specimen (span)

r_B = radius of bend specimen

σ_0 = constant.

In the rotating-beam fatigue test, all poritions of the specimen at the same radial position in the gage section are subject to about the same tensile stress, and the effective risk of rupture, R_F, may be computed as follows, with V the specimen volume that is subject to tension during a fatigue cycle, r_F the radius of the fatigue specimen, and ℓ_F its length:

$$R_F = \int_V \left(\frac{\sigma}{\sigma_0}\right)^m dV$$

$$\sigma = \frac{r}{r_F}\sigma_F$$

$$dV = \ell_F 2\pi r\, dr$$

$$0 \le r \le r_F$$

$$R_F = \left(\frac{\sigma_F}{\sigma_0}\right)^m \frac{2\pi r_F^2 \ell_F}{(m+2)} .$$

The expected relative strengths of the "mate" and fatigue specimens, σ_B/σ_F, may be obtained by equating R_B and R_F:

$$\frac{\sigma_B}{\sigma_F} = \left[\frac{\Gamma\left(\frac{m}{2}+1\right)}{\Gamma\left(\frac{m+1}{2}\right)}(m+1)\,2\sqrt{\pi}\left(\frac{\ell_F r_F^2}{\ell_B r_B^2}\right)\right]^{1/m} .$$

For the effective volume assumed to be under uniform stress in the fatigue specimen, we take the straight-gage-section volume where ℓ_F = 1/8 in. and r_F = 0.2 in., while for the "mate" in three-point bending ℓ_B = 2.375 in. and r_B = 0.25 in.

Using m = 9 from the strength distribution (Fig. 7), we get

$$\frac{\sigma_B}{\sigma_F} = \left[\frac{\Gamma(5.5)}{\Gamma(5)}(10)(3.54)\left(\frac{0.64}{19}\right)\right]^{1/9}$$

$$\frac{\sigma_B}{\sigma_F} = 1.112.$$

The expected first-cycle strength of the fatigue specimens is then 90% of the strength of the bending "mates" for the material and fatigue-specimen configuration used here. The value σ_B is the bending strength of the "mate," and the relation between the two expresses the effect of geometric differences as well as size, since in rotating, all portions of the fatigue specimen are subject to tension.

The stress ratio plotted in the homologous stress graph (Fig. 3a) is the applied stress divided by 0.9 times the "mate" bending strength, giving the ratio of operational stress to expected first-cycle strength of the fatigue samples. In Fig. 3b the average of all 50 "mates" is corrected for size by the factor 0.9, and this value is used as the estimate of first-cycle strength of all fatigue specimens.

APPENDIX B

CALIBRATION OF FATIGUE-TESTING EQUIPMENT

The Krouse fatigue machine used in these tests was designed primarily for testing metal specimens and thus was originally rated at approximately 200 in.-lb maximum capacity. Since it was known that the graphite fatigue specimens would be tested at the lower end of the scale, a smaller spindle

assembly was substituted for that originally supplied with the machine. For these reasons, and also because the graphite fatigue specimens were not of the usual design, it was necessary to calibrate the equipment in order to determine accurately the applied bending moment.

As outlined under "Specimens and Test Procedure," the desired moment was set on the lever arm of the test machine. This was done by testing a 1/4 in. by 1/4 in. steel beam of the same length as the graphite test specimen, with two SR-4 strain gages mounted on opposite surfaces of the beam and at the same relative position as the reduced section of the graphite fatigue specimen (see Fig. 8).

To translate strain-gage readings to bending moment, it was first necessary to determine the modulus of elasticity of the mild steel beam by applying a known moment. First, the distance between the center of gravity of the spindle assembly and the reduced section (strain gages on steel beam) was determined to be 4.83 in. (as shown in Fig. 9). Using the spindle assembly only, a known moment could then be applied to the steel calibration beam mounted in the test machine. E_s, the modulus of elasticity of the steel beam, was then found by the cantilever beam equation

$$E_s = \frac{6wd}{bh^2\epsilon_s} = \frac{6 \times 1.685 \times 4.83}{(0.25)^3 \times 112 \times 10^{-6}}$$

$$= 27.8 \times 10^6 \text{ lb/in.}^2$$

where w = weight of spindle assembly (including bearing and cage)

d = distance (in inches) between strain gages and center of gravity of spindle assembly

ϵ_s = strain in steel beam in in./in.

b and h = cross-sectional dimensions of steel beam (0.25 in.^{2}).

An expression relating the strain-gage reading to the maximum fiber stress in the reduced section of the graphite specimen is derived as follows:

The stress in the steel specimen is

$$\sigma_s = \frac{MC}{I} = \frac{6M}{bh^2} .$$

The maximum fiber stress in the reduced section of the graphite specimen is

$$\sigma_g = \frac{MC}{I} = \frac{32M}{\pi D^3}$$

where D = diameter of reduced section of graphite specimen (0.20 in.). The moments are equal, therefore

$$\frac{\sigma_s bh^2}{6} = \frac{\sigma_g D^3}{32}$$

and, since $\sigma = \epsilon E$

$$\epsilon_s = \frac{3\pi D^3 \sigma_g}{16 E_s bh^2} . \qquad \text{(B-1)}$$

Equation (B-1) reduces to

$$\epsilon_s = 0.01087\ \sigma_g/\mu\text{in./in.} \qquad \text{(B-2)}$$

where σ_g is expressed in lb/in.^{2}.

Figure 10 shows the indicated moment setting (the setting of the sliding weight on the lever arm) plotted against the strain-gage readings. This figure was used to determine an initial approximate moment setting before the final fine adjustment of the sliding weight was made. Note that a zero moment setting results in a negative moment on the specimen.

APPENDIX C

STATISTICAL ANALYSIS OF FATIGUE DATA

It is an experimental fact that fatigue-life is a highly variable quantity which demands some processing to make it tractable, even statistically. The usual first step is to consider as the variable, not the life in cycles, but the logarithm of N, the number of cycles to failure. This reduces drastically the numerical range of the variable, but even so the data remain highly variable. The purpose of a statistical description is to estimate low-probability contours for high-reliability design predictions.

For convenience a Weibull distribution was used in this experiment to fit the lifetime data. This distribution was of the form normalized to the mean value:

$$S = \exp\left(-\frac{L}{\overline{L}}\right)^m \left[\Gamma\left(1+\frac{1}{m}\right)\right]^m \qquad \text{(C-1)}$$

where S is the probability that life will exceed L, L is $\log_{10} N$, $\overline{L}$ is the average of L, m is the Weibull Modulus (to be estimated), and Γ is the gamma function.

When $\overline{L}$ and m are known, the probability of failure, 1 - S, can be found. Both $\overline{L}$ and m vary as the fatigue stress changes. The average life $\overline{L}$ will of course increase as the stress is reduced, while our data indicate that m decreases with decreasing fatigue stress (Table 3 and Fig. 11).

Lipson *et al.*[11] have summarized a wide variety of metal-fatigue data which they fitted with Weibull distributions. They propose methods of transforming life variability to stress variability at constant life, and give

the Weibull parameters as functions of life from 10^3 to 10^7 cycles. It is interesting to note that the variance of the metal-fatigue results exceeds that of the present experiment and, at high lifetimes, the homologous stress capability is lower. Their values of m range from about 1.5 to 4.

The estimation of the Weibull modulus can follow a variety of methods, all of which are of roughly equal merit.[12] When the average value cannot be calculated from the data (i.e., when some specimens in a group have not been tested to failure) the approach used here was to transform Eq. (C-1):

$$\log \ln \frac{1}{S} = m \log L + \log \left(\frac{\Gamma^m}{\bar{L}} \right). \qquad \text{(C-2)}$$

The observed failures at L and the corresponding probabilities S define a straight line (ideally) on logarithmic coordinates, the slope of which is the desired parameter m. Such a plot also allows estimation of the mean value since, now that m is known, the probability of survival S at the mean is simply a function of m:

$$S_{mean} = \exp \left[\Gamma \left(1 + \frac{1}{m} \right) \right]^m . \qquad \text{(C-3)}$$

It is known that fatigue data from a variety of similar materials can be correlated by using a normalized stress in place of the absolute stress in the usual S/log-N diagram. The applied fatigue stress is normalized by dividing by the strength of the test specimen. When the strength is extremely variable, as for graphite, the normalization must consider effects of size and stress distribution, discussed in Appendix A, as well as the implications of statistical variability. To determine the effect of the latter, the strength was estimated in two ways: first, from the sample average of the series of strength tests, and second, by maintaining an identification between the fatigue

specimens and those used for short-time strength-testing. Each pair of specimens, one for fatigue testing and one for short-time bend-testing, was cut from a single 6-in.-long rod. The strength of the bend specimen constituted an estimate of the true strength of its mating fatigue specimen. The results show that "mate" strength, as an individual normalizing factor, gives slightly better correlation of the data than does the total sample average (see Fig. 3c).

This appendix describes the method of analyzing the data and the processing of all the observations from both standpoints ("mate" strength and sample average).

The fatigue data were first tabulated as ordered sets on stress parameter (Tables 4 and 11), and then plotted as frequency histograms (Figs. 12 and 14) to aid in grouping. Once grouped according to stress, the observed failures in each group were ranked according to fatigue life, the probabilities were computed, and the data were analyzed graphically to be fit by a Weibull function (Fig. 14). The results were used to plot the 50% and the 10% probability-of-failure contours on stress-parameter vs time coordinates. It should be noted again that failures within one cycle are essentially static tests that serve in effect as proof tests. Clearly all specimens that exhibited some fatigue life had a first-cycle strength exceeding the fatigue level, and it is expected that in a sufficient sample, occasional static failures will occur (as were observed) because of insufficient strength. The incidences and expectations for such fractures are shown in the data tables.

Table 4 is a summary of all the data using homologous stress based on "mate" strength; it gives the grouping

selected on the basis of the frequency plot of Fig. 12. Tables 5 through 10 list the data for each of these groups. The values for "mate" strength, found by multiplying the measured strength of the "mate" by the size-effect factor 0.9, are estimates of the expected first-cycle strength of each fatigue specimen. The normalized log life values are found by dividing each log life by the average log life. The fatigue life distribution of each group was approximated by a Weibull distribution and plotted in Fig. 13. Since some observations exceeded the greatest observed life (run-outs), the true mean value did not, in such cases, correspond with the sample-average fatigue life. In these cases the Weibull modulus was estimated first from the slope of the best straight line on suitable log-log coordinates, and the average value was estimated from the probability corresponding to the mean value at the estimated Weibull modulus.

The homologous stress for each specimen in Tables 5 through 10 is based on the strength of its mate. An alternate approach is to use the total sample average as a normalizing factor. This approach is described in Tables 11 through 15. The control variable is simply the applied fatigue stress, and the method of grouping and statistical analysis follows the previously used scheme. A frequency diagram (Fig. 14) was used to define the groups, each of which is then analyzed in Tables 12-15. Since the total sample average of the bending tests was 15,000 psi, the expected first-cycle strength in fatigue was estimated by invoking the size-effect correction, 0.9, to get 13,500 psi. The applied stresses were normalized by this value to get the plots on Figs. 3b and 3c. A summary of the life distributions obtained by this grouping is shown in Fig. 15.

The experimental data, comprising 6 to 9 specimens per group, provide a reasonable basis for locating the 10% failure probability contour but are not suitable for extrapolation to very low values such as 1%. The plot of Fig. 3c shows the similarity of results derived from both analyses (homologous stress and absolute stress) and suggests that the variability of stress at constant life is low and relatively constant. Accordingly, in order to estimate the 1% failure probability the data were approximated by a Weibull distribution of stress at constant life. The ratio of the stresses at 10% failure probability to the stresses at 50% failure probability was found to be about 0.86 and fairly uniform. The method of estimating the Weibull modulus is as follows: We have, using β as the normalized variable,

$$S = e^{-\beta^m \Gamma^m}$$

$$\ln \frac{1}{S} = \beta^m \Gamma^m$$

and from two pairs of S and β we get

$$m = \left(\frac{1}{\ln \frac{\beta_1}{\beta_2}} \right) \ln \left\{ \frac{\ln \frac{1}{S_1}}{\ln \frac{1}{S_2}} \right\} .$$

For $S_1 = 0.90$ and $S_2 = 0.5$

$$m = \ln \left(\frac{1}{\ln (0.86)} \right) \left(\frac{\ln 1.111}{\ln 2} \right)$$

and, finally,

$$\underline{m = 12.5}.$$

Assuming now that the "vertical" distribution on Fig. 3 is everywhere described by a Weibull distribution with the above modulus, we can plot additional probability contours such as the 1% level shown on the graph.

REFERENCES

[1]W. M. Wells et al., High-Temperature Testing of Graphite Helical-Screw Expanders and Compressors, Lawrence Radiation Laboratory, Livermore, Rept. UCRL-14660 (1966).

[2]L. Green, "The Behavior of Graphite under Alternating Stress," J. Appl. Mech. 18, 345-48 (1951).

[3]Cited in General Electric Pyrolytic Graphite Engineering Handbook.

[4]J. W. Dally, Design Data for Materials Employed in Thermal Protective Systems on Advanced Aerospace Vehicles, Air Force Tech. Doc. Report ML-TDR-64-204, Vol. 3 (August 1965).

[5]L. L. France and V. Kachur, "Mechanical Behavior of a Continuous Filament Carbon Composite," American Institute of Aeronautics and Astronautics, 5th Aerospace Sciences Meeting, New York, 1967. AIAA Paper No. 67-173.

[6]V. N. Barabanov, Yu. P. Anufriev, G. G. Zaitsev, and M. Ya. Pimkin, "Some Special Features of the Method of Testing Graphite for Fatigue in Alternate-Reverse Bending, and the Results Obtained," Zavodskaya Laboratoriya, Industrial Laboratory (English transl.) 32, 459-62 (1964).

[7]I. C. Lipson, N. J. Sheth, and R. L. Disney, Reliability Prediction—Mechanical Stress/Strength Interference, University of Michigan, Ann Arbor, Tech. Rept. RADC-TR-66-710 (March 1966).

[8]J. E. Campbell, F. J. Barone, and D. P. Moon, The Mechanical Properties of the 18% Nickel Maraging Steels, Defense Metals Information Center, Battelle Memorial Institute, Columbus, Ohio, Report No. 198 (1964).

[9]Mechanical Properties of Engineering Ceramics, Proceedings of a Conference on the Mechanical Properties of Engineering Materials, Raleigh, North Carolina, 1960, W. W. Kriegel and H. Palmour III, Eds. (Interscience, N. Y., 1961), p. 260; also see Ref. 6.

[10]E. Robinson, Some Theoretical and Experimental Aspects of Design with Brittle Materials, Lawrence Radiation Laboratory, Livermore, Rept. UCRL-7729 (1964).

[11]I. C. Lipson, N. J. Sheth, and R. L. Disney, Reliability Prediction—Mechanical Stress/Strength Interference, University of Michigan, Ann Arbor, RADC-TR-66-710 (March 1966).

[12]E. Robinson, Some Problems in the Estimation and Application of Weibull Statistics, Lawrence Radiation Laboratory, Livermore, Rept. UCRL-70555 (September 1, 1967).

Table 1. "Mate" strength analysis of EP-1924 graphite. 50 specimens tested; average strength = 15,000 psi. Strengths are normalized to sample or mode average.

Fraction of average strength					
Unimodal analysis	Multimode analysis (first mode)	Unimodal analysis	Multimode analysis (second mode)	Unimodal analysis	Multimode analysis (third mode)
0.753	0.892	0.953	0.925	1.150	0.975
0.753	0.892	0.966	0.935	1.166	0.988
0.773	0.915	0.986	0.955	1.173	0.994
0.780	0.925	0.986	0.955	1.186	1.005
0.813	0.965	1.	0.97	1.200	1.017
0.833	0.987	1.	0.97	1.213	1.028
0.840	0.995	1.013	0.98	1.226	1.037
0.846	1.	1.020	0.99		
0.860	1.02	1.020	0.99	$\frac{\text{Third mode av}}{\text{Sample av}} = 1.18$	
0.860	1.02	1.020	0.99		
0.880	1.04	1.020	0.99		
0.893	1.06	1.026	0.995		
0.900	1.065	1.033	1.		
0.900	1.065	1.046	1.01		
0.906	1.07	1.046	1.01		
0.920	1.09	1.046	1.01		
		1.046	1.01		
$\frac{\text{First mode av}}{\text{Sample av}} = 0.845$		1.060	1.03		
		1.073	1.04		
		1.073	1.04		
		1.093	1.06		
		1.093	1.06		
		1.1	1.065		
		1.1	1.065		
		1.106	1.07		
		1.113	1.08		
		1.120	1.086		
		$\frac{\text{Second mode av}}{\text{Sample av}} = 1.03$			

Table 2. Results of Multi-mode Analysis

	Fraction of sample	$\frac{\text{Mode av}}{\text{Total sample av}}$	Weibull modulus of each mode
Low mode	0.32	0.845	18
Middle mode	0.54	1.03	30
High mode	0.14	1.185	50

Table 3. Homologous stress based on "mate" strength vs Weibull modulus m, and the 50% and 10% probability points.

Group	Homologous stress	Sample size	Weibull modulus m		50% life cycles	10% life cycles
			av.	Std. dev.		
I	0.9	9	4.5	1.5	23	8
II	0.78	6	4.5	1.8	110	21
III	0.73	6	3.5	1.9	1000	63
IV	0.71	5	2	0.89	9250	37
V	0.66	7	2	0.76	$2.2(10^5)$	110
VI	0.61	3	1.5[a]	0.87	$3(10^{15})$	$3(10^4)$

[a]Estimated by extrapolation of m vs homologous stress (see Fig. B-1).

Table 4. Summary of homologous stress data based on "mate" strength, grouped on the basis of the frequency plot of Fig. B-2.

Group	Homologous stress	Life cycles
I	0.954	9
	1.00	a
	0.913	45
	0.906	a
	0.900	16
	0.896	16
	0.896	13
	0.890	39
	0.889	a
	0.885	25
	0.883	a
	0.880	130
	0.845	6
II	0.828	a
	0.797	150
	0.797	28
	0.779	350
	0.775	80
	0.775	28
	0.761	250
III	0.750	4800
	0.740	$1.3 \times 10^8 \rightarrow$
	0.740	40
	0.725	100
	0.723	500
	0.723	2000
IV	0.711	2×10^5
	0.700	50
	0.700	140
	0.700	$1.2 \times 10^7 \rightarrow$
	0.695	1.1×10^4
	0.695	6×10^7
	0.68	a
V	0.667	700
	0.667	500
	0.661	2×10^4
	0.661	$1.5 \times 10^8 \rightarrow$
	0.654	10^7
	0.650	$4.5 \times 10^7 \rightarrow$
	0.645	8×10^5
VI	0.619	1.05×10^7
	0.614	5×10^8 [b] →
	0.600	$2 \times 10^7 \rightarrow$

[a] Failed during first cycle.

[b] Motor failure.

Table 5. Fatigue-life probability distribution for homologous stress data based on "mate" strength, Group I data from Table B-II. Homologous stress range = 0.845 to 0.913, av = 0.895. Number in group = 9, number failed = 9.

Rank	Observed life cycles	Log life	Normalized log life	Upper bound of cumulative failure probability
1	6	0.777	0.582	0.11
2	9	0.954	0.715	0.22
3	13	1.114	0.835	0.33
4	16	1.204	0.903	0.44
5	16.1	1.205	0.904	0.55
6	25	1.398	1.05	0.66
7	39	1.591	1.19	0.77
8	45	1.653	1.24	0.88
9	130	2.114	1.58	1.

Estimated mean log life = 1.34, m = 4.5.

Forecasts

Failure probability	Log life	Life cycles	Failure probability at this homologous stress	First-cycle failures	
				Predicted	Observed
50%	1.36	23	0.21	2	4
10%	0.89	8			

Table 6. Fatigue-life probability distribution for homologous stress data based on "mate" strength, Group II data from Table B-II. Homologous stress range = 0.76 to 0.795, av = 0.78. Number in group = 6, number failed = 6.

Rank	Observed life cycles	Log life	Normalized log life	Upper bound of cumulative failure probability
1	28	1.45	0.73	0.167
2	29	1.46	0.73+	0.33
3	80	1.9	0.95	0.5
4	150	2.18	1.1	0.67
5	250	2.4	1.2	0.83
6	350	2.54	1.28	1.

Estimated mean log life = 2, m = 4.5.

Forecasts

Failure probability	Log life	Life cycles	Failure probability at this homologous stress	First-cycle failures	
				Predicted	Observed
50%	2.04	110	0.06	0.96	1
10%	1.32	21			

Table 7. Fatigue-life probability distribution for homologous stress data based on "mate" strength, Group III from Table B-II. Homologous stress range = 0.72 to 0.75, av = 0.73. Number in group = 6, number failed = 5.

Rank	Observed life cycles	Log life	Normalized log life	Upper bound of cumulative failure probability
1	40	1.60	0.53	0.167
2	100	2.0	0.67	0.33
3	500	2.70	0.9	0.5
4	2200	3.30	1.1	0.67
5	4800	3.68	1.23	0.83
6	$1.3\ (10^8) \rightarrow$	—	—	—

Estimated mean log life = 3, m = 3.5.

Forecasts

Failure probability	Log life	Life cycles	Failure probability at this homologous stress	First-cycle failures	
				Predicted	Observed
50%	3.00	1000	0.2	1.2	0
10%	1.80	63	0.03	0.18	

Table 8. Fatigue-life probability distribution for homologous stress data based on "mate" strength, Group IV data from Table B-II. Homologous stress range = 0.68 to 0.71, av = 0.70. Number in group = 6, number failed = 5.

Rank	Observed life cycles	Log life	Normalized log life	Upper bound of cumulative failure probability
1	50	1.7	0.402	0.2
2	140	2.28	0.54	0.4
3	1.1 (10^4)	4.04	0.96	0.6
4	2.0 (10^5)	5.301	1.26	0.8
5	1.2 (10^7)→ [a]	—	—	—
6	6.04 (10^7)	7.78	1.84	1.0

. Estimated mean log life = 4.22, m = 2.

Forecasts

Failure probability	Log life	Life cycles	Failure probability at this homologous stress	First-cycle failures	
				Predicted	Observed
50%	3.97	9250	0.02	0.12	1
10%	1.56	37			

[a]Not used in analysis.

Table 9. Fatigue-life probability distribution for homologous stress data based on "mate" strength, Group V data from Table B-II. Homologous stress range = 0.645 to 0.67, av = 0.66. Number in group = 7, number failed = 5.

Rank	Observed life cycles	Log life	Normalized log life	Upper bound of cumulative failure probability
1	500	2.69	0.47	0.143
2	700	2.84	0.5	0.283
3	1.97 (10^4)	4.29	0.75	0.43
4	7.96 (10^5)	5.90	1.03	0.56
5	10^7	7.0	1.23	0.71
6	14.5 (10^7)→	—	—	—
7	1.48 (10^8)→	—	—	—

Estimated mean log life = 5.7, m = 2.

Forecasts

Failure probability	Log life	Life cycles	Failure probability at this homologous stress	First-cycle failures	
				Predicted	Observed
50%	5.35	2.2 (10^5)	0.01	0.07	0
10%	2.10	110			

Table 10. Fatigue-life probability distribution for homologous stress data based on "mate" strength, Group VI data from Table B-II. Homologous stress range = 0.60 to 0.62, av = 0.61. Number in group = 3, number failed = 1.

Rank	Observed life (cycles)	Log life
1	1.05 (10^7)	7.0
2	2.06 (10^7)→	–
3	5 (10^8)→	–

Assumed Weibull modulus m = 1.5.

Estimated mean log life ≈ 18.

Forecasts		
Failure probability	Log life	Life cycles
50%	15.5	3 (10^{15})
10%	4.50	3 (10^4)

Table 11. Summary of homologous stress data based on total sample average, grouped on the basis of the frequency plot of Fig. B-3.

Group	Max stress (units of 10^3 psi)	Observed life cycles
I	15.0	39
	12.7	16
	12.3	a
	12.3	13
	12.3	130
	11.8	28
II	11.35	25
	11.25	a
	11.25	50
	11.2	45
	11.2	80
	11.2	150
	11.05	28
	10.55	a
III	10.25	a
	10.25	a
	10.25	a
	10.25	6
	10.25	16
	10.25	40
	10.25	100
	10.25	250
	10.25	4800
	10.25	$2\ (10^4)$
	10.25	10^7
	10.25	$1.05\ (10^7)$
	10.03	700
	9.9	$6\ (10^7)$
	9.8	9
IV	9.65	$1.3\ (10^8)\rightarrow$
	9.65	140
	9.65	350
	9.6	500
	9.6	2000
	9.6	$2\ (10^5)$
	9.6	$4.5\ (10^7)\rightarrow$
	9.55	$1.1\ (10^4)$
	9.55	$8\ (10^5)$
	9.4	500 (flaw)
V	8.95	$1.2\ (10^7)\rightarrow$
	7.65	$1.5\ (10^8)\rightarrow$
	6.25	$2\ (10^7)\rightarrow$
	6.25	$5\ (10^8)$ b
	6.0	$1.5\ (10^7)$

[a]Failed during first cycle.
[b]Motor failed.

Table 12. Fatigue-life probability distribution for homologous stress data based on total sample average, Group I data from Table B-IX. Stress range = 11.8 to 15, av = 12.8 (units of 10^3psi). Number in group = 5, number failed = 5.

Rank	Observed life cycles	Log life	Normalized log life	Upper bound of cumulative failure probability
1	13	1.11	0.67	0.2
2	16	1.2	0.81	0.4
3	28	1.44	0.97	0.6
4	39	1.6	1.07	0.8
5	130	2.1	1.41	1

Estimated mean log life = 1.49, m = 4.

Forecasts

Failure probability	Log life	Life cycles	Failure probability at this homologous stress (0.95)	First-cycle failures	
				Predicted	Observed
50%	1.50	32	0.32	1.5	1
10%	0.94	9		1.6	

Table 13. Fatigue-life probability distribution for homologous stress data based on total sample average, Group II data from Table B-IX. Stress range = 11.05 to 11.35, av = 11.2 (units of 10^3 psi). Number in group = 6, number failed = 6.

Rank	Observed life cycles	Log life	Normalized log life	Upper bound of cumulative failure probability
1	25	1.40	0.82	0.167
2	28	1.45	0.85	0.33
3	45	1.65	0.96	0.5
4	50	1.70	0.99	0.67
5	80	1.90	1.11	0.83
6	150	2.18	1.27	1

Estimated mean log life = 1.713, m = 7.

Forecasts

Failure probability	Log life	Life cycles	Failure probability at this homologous stress (0.83)	First-cycle failures	
				Predicted	Observed
50%	1.72	52	0.11	0.66	2
10%	1.31	20			

Table 14. Fatigue-life probability distribution for homologous stress data based on total sample average, Group III data from Table B-IX. Stress range = 9.8 to 10.3, av = 10.2 (units of 10^3 psi). Number in group = 12, number failed = 12.

Rank	Observed life cycles	Log life	Normalized log life	Upper bound of cumulative failure probability
1	6	0.78	0.225	0.083
2	9	0.95	0.27	0.17
3	16	1.2	0.35	0.25
4	40	1.6	0.46	0.33
5	100	2	0.58	0.42
6	250	2.4	0.69	0.5
7	700	2.84	0.82	0.58
8	4800	3.68	1.06	0.67
9	2 (10^4)	4.3	1.24	0.75
10	10^7	7	2.02	0.83
11	1.05 (10^7)	7.02	2.03	0.92
12	6 (10^7)	7.78	2.25	1

Estimated mean log life = 3.46, m = 1.3.

Forecasts

Failure probability	Log life	Life cycles	Failure probability at this homologous stress (0.76)	First-cycle failures	
				Predicted	Observed
50%	2.85	690	0.5	0.6	3
10%	0.70	5	0.05		

Table 15. Fatigue-life probability distribution for homologous stress data based on total sample average, Group IV data from Table B-IX. Stress range = 9.4 to 9.65, av = 9.6 (units of 10^3 psi). Number in group = 10, number failed = 8.

Rank	Observed life cycles	Log life	Normalized log life	Upper bound of cumulative failure probability
1	140	2.14	0.5	0.1
2	350	2.54	0.59	0.2
3	500	2.7	0.63	0.3
4	500	2.7	0.63	0.4
5	2000	3.30	0.77	0.5
6	1.1 (10^4)	4.04	0.94	0.6
7	2 (10^5)	5.3	1.23	0.7
8	8 (10^5)	5.9	1.37	0.8
9	4.5 (10^7)→	7.65	1.78	—
10	1.3 (10^8)→	8.11	1.89	—

Estimated mean log life = 4.3, estimated m = 2.3.

Forecasts

Failure probability	Log life	Life cycles	Failure probability at this homologous stress (0.71)	First-cycle failures	
				Predicted	Observed
50%	4.12	13,400	0.03	0.3	0
10%	1.85	71			

FIGURE CAPTIONS

Fig. 1. Graphite fatigue-test specimen.

Fig. 2. Fatigue-test apparatus. (a) Arranged for calibration, with the steel calibration beam in place; the strain readout unit is at the right. (b) Fatigue test in progress.

Fig. 3. S-N plots of EQ-1924 graphite fatigue-life data, with 50%, 10%, and 1% failure probability contours. Rotating beam tests at room temperature; 10,000 cycles/min, R = -1. (a) Homologous stress based on "mate" strength. (b) Homologous stress based on total sample average. The curves are calculated probabilities of failure. (c) Plot of 50% and 10% failure probability points for both kinds of homologous stress data. The 50% and 10% contours are from the statistical analysis of the data. The 10% contours were constructed analytically. The open symbols indicate runout (no failure) data.

Fig. 4. Three fatigue fractures, showing flaws. Applied stress, homologous stress (sample average), and life in number of cycles were, respectively: (a) 10,500, 0.78, <1; (b) 11,350, 0184, 25; (c) 9400, 0.70, 500.

Fig. 5. Generalized correlation of graphite fatigue data. The open symbols indicate runout (no failure) data.

Fig. 6. Strength probability distributions for the three modes, derived from bending tests of the "mate" specimens.

Fig. 7. Results of the three-point bending test of the "mate" specimens. Dashed curve: Weibull distribution with m = 9. Solid curve: multimode analysis, with the three modes characterized as shown in Table 2.

Fig. 8. Strain-gaged steel beam (arrow) mounted in the fatigue machine.

Fig. 9. Diagram illustrating the procedure for determining the position of the center of gravity of the spindle assembly. With a knife edge placed at point B in the center of the steel specimen to act as a fulcrum, enough weight was added at point A to balance the assembly. With a known weight at point A, a known weight of spindle assembly, and a known distance A-B, we obtain $\bar{x}$, the distance from point B to the center of gravity of the spindle assembly: $x = (2336.6/766)(1.3) = 3.965$ in.

Fig. 10. Strain-gage reading vs indicated moment.

Fig. 11. Weibull modulus vs homologous stress (based on "mate" strength) for the six groups described in Table 3, showing how the m value for Group VI (arrow) was estimated by extrapolation. The bars indicate ±1 standard deviation.

Fig. 12. Frequency grouping of homologous stress data based on "mate" strength.

Fig. 13. Probability of failure vs normalized log life from the homologous stress data based on "mate" strength, for five of the six groups summarized in Fig. 12 and Table 4: Group I (Table 5), Group II (Table 6), Group III (Table 7), Group IV (Table 8), Group V (Table 9).

Fig. 14. Frequency grouping of data according to applied fatigue stress.

Fig. 15. Probability of failure vs normalized log life from the homologous stress data based on total sample average, for the four groups summarized in Fig. 13 and Table 11: Group I (Table 12), Group II (Table 13), Group III (Table 14), Group IV (Table 15). Mean stress is in units of 10^3 psi.

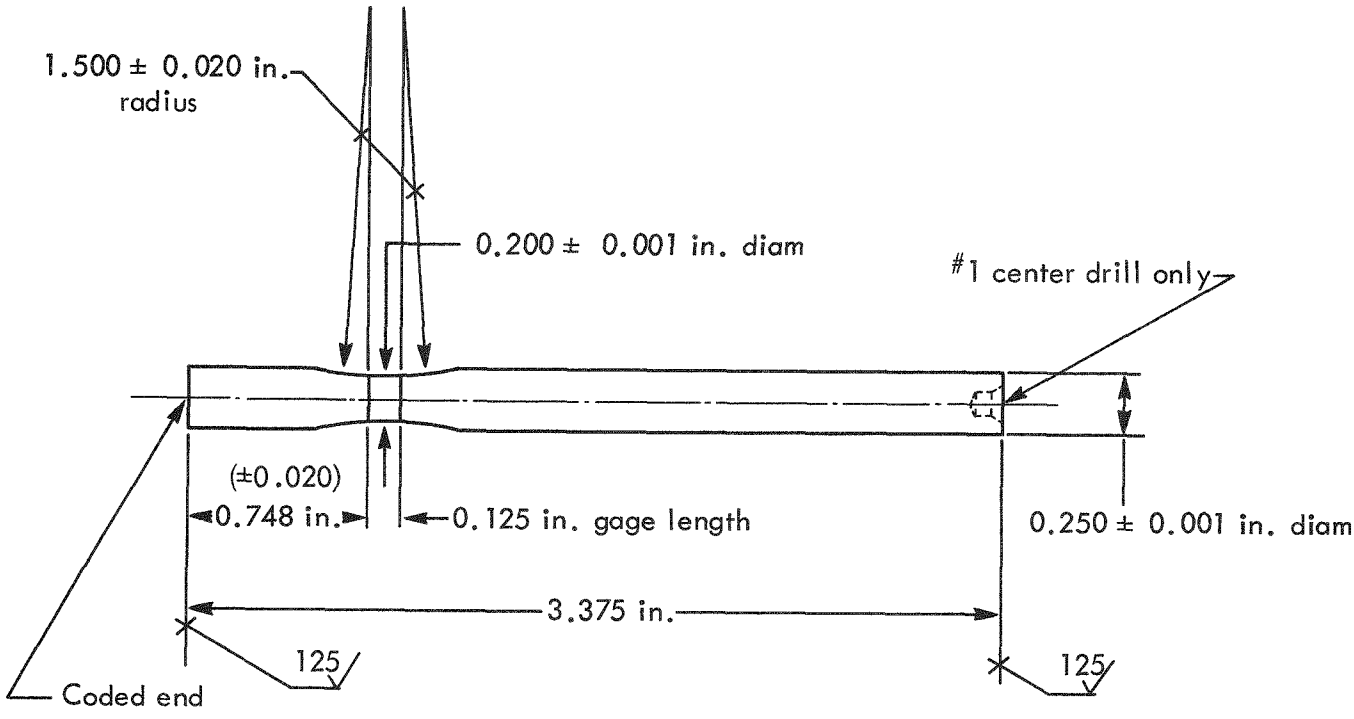

Notes: 1. 16/ FAO and polish to a high luster unless otherwise specified.
2. All diameters concentric within 0.0005 in.
3. 1.500 in. radius to be tangent to 0.200 ± 0.001 in. diam.

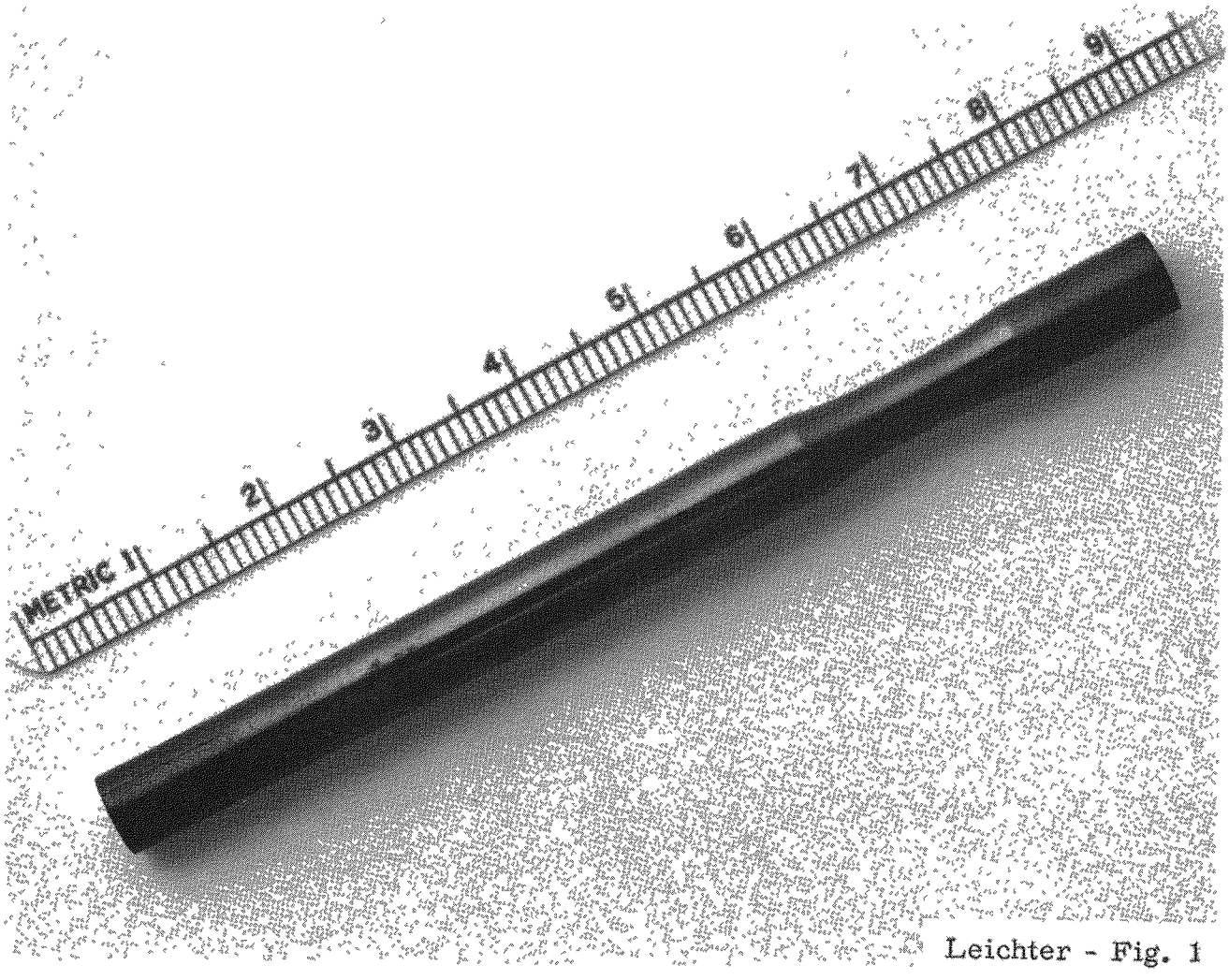

Leichter - Fig. 1

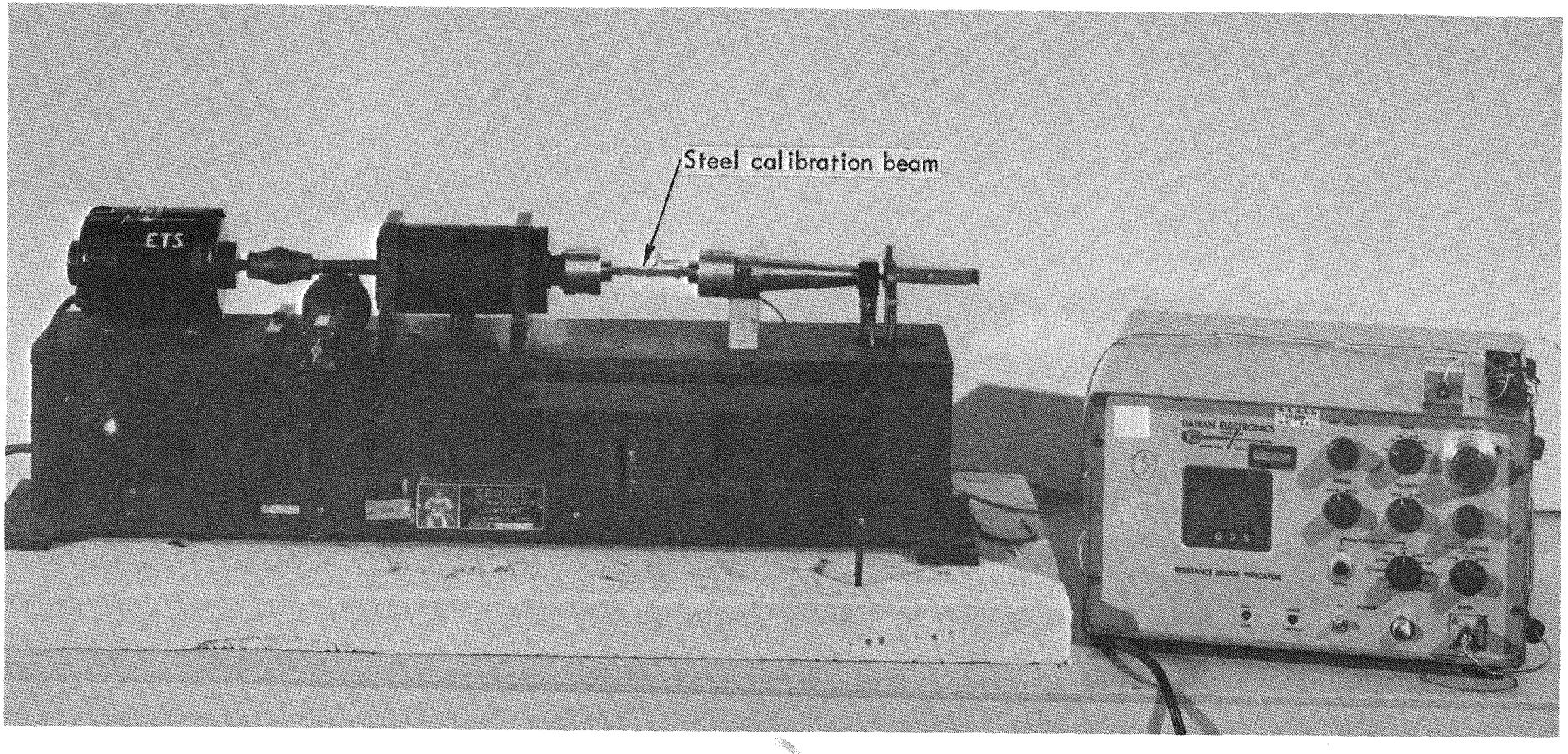

(a)

Leichter - Fig. 2a

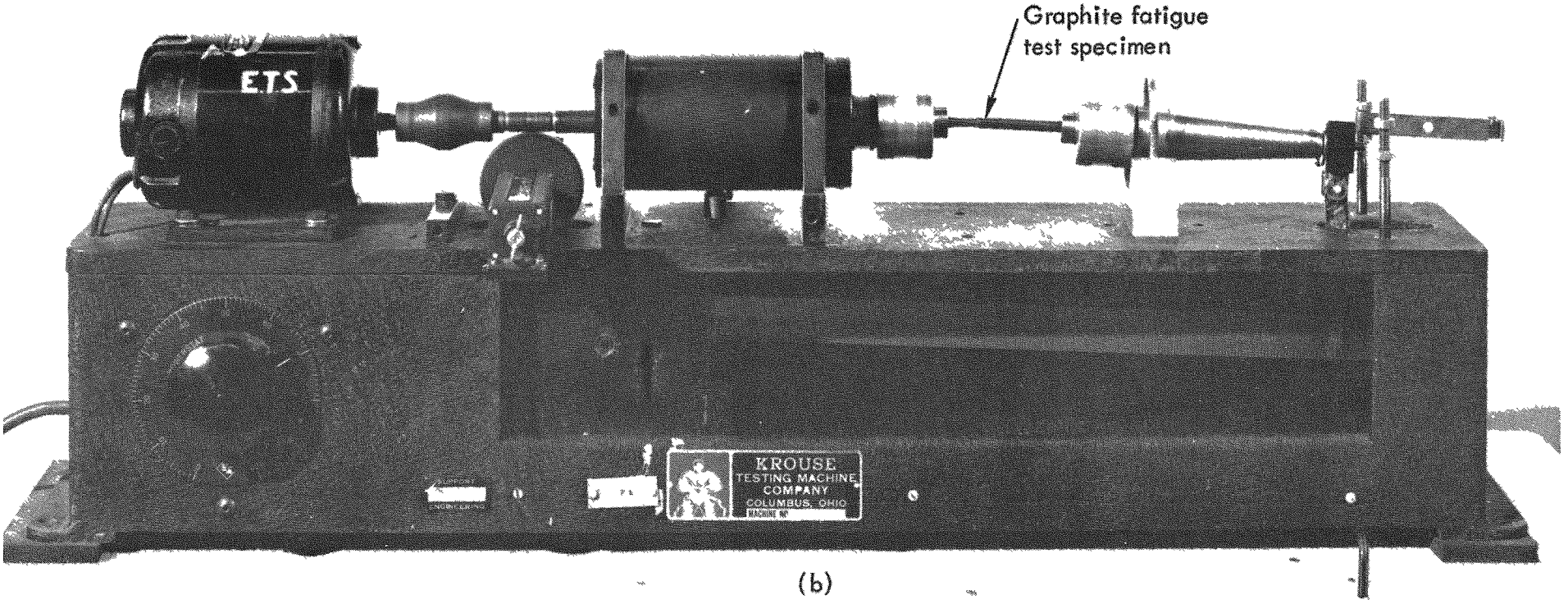

(b)

Leichter - Fig. 2b

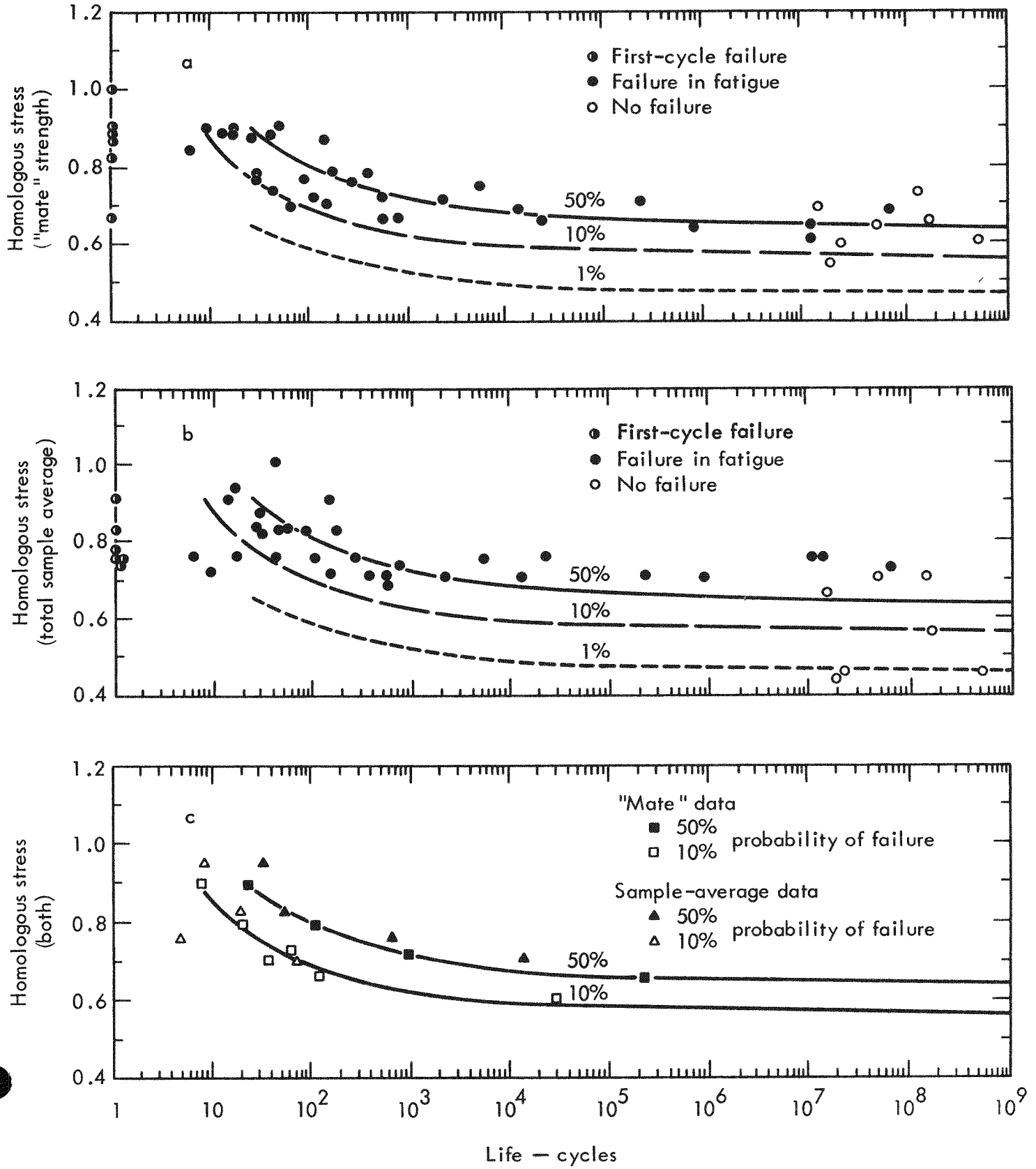

Leichter - Fig. 3

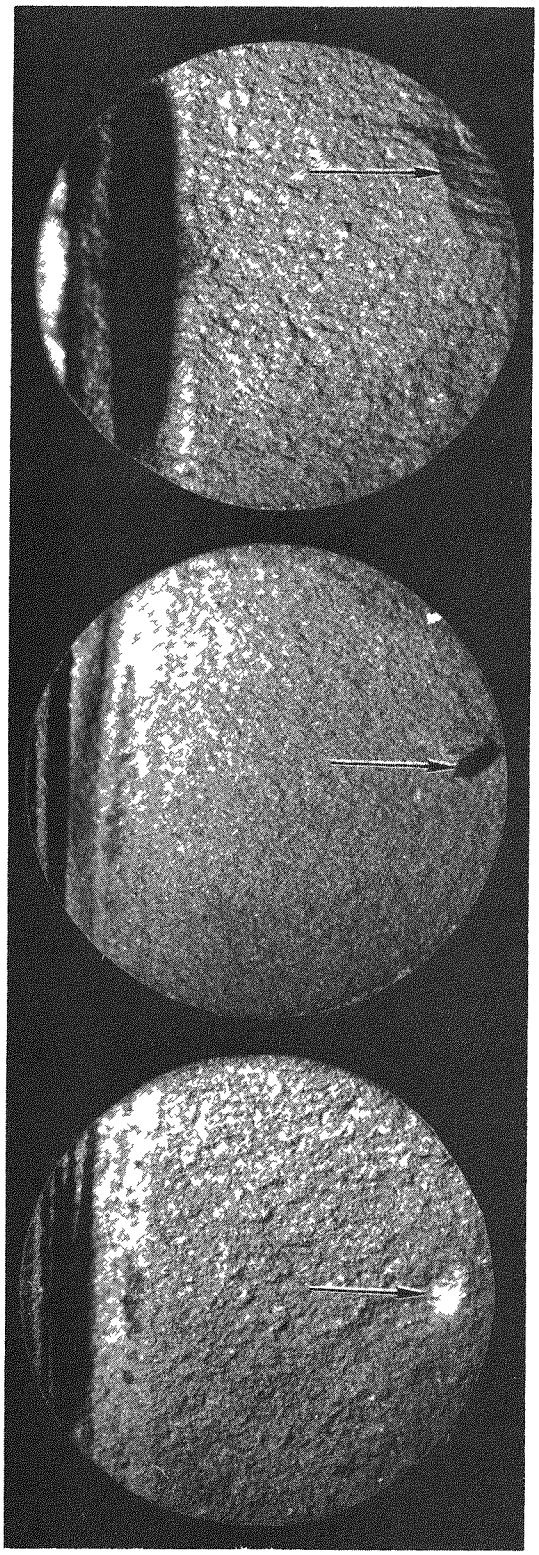

Leichter - Fig. 4

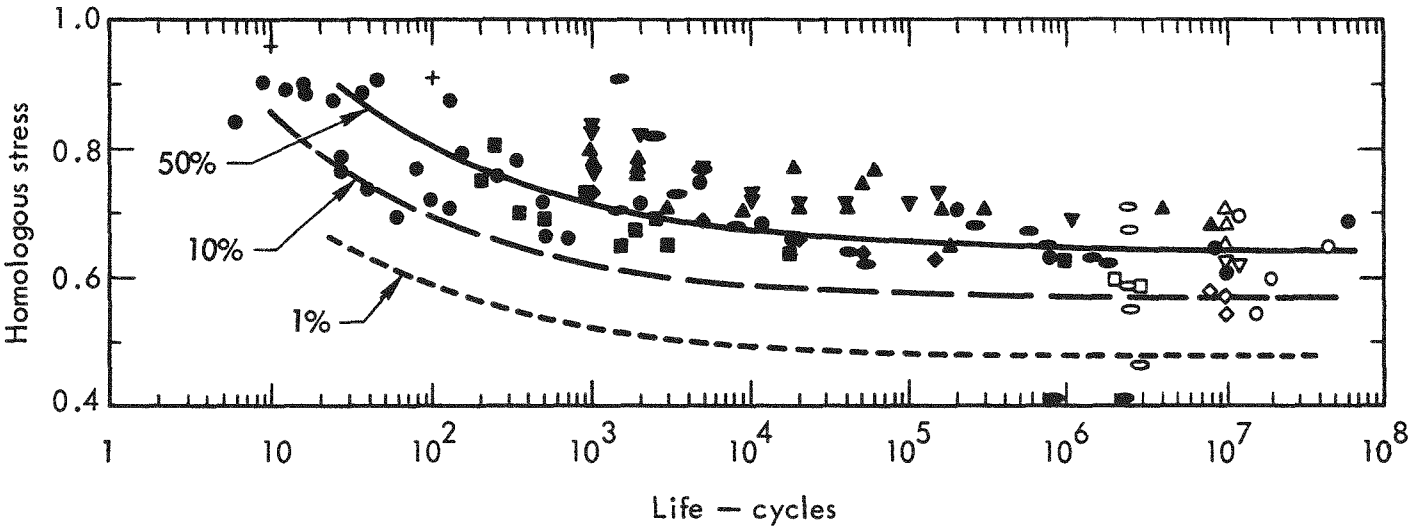

	Reference	Material	Av strength (psi)
●	Leichter and Robinson, this report	AXF	13,500
◆	France and Kachur [5]	Carbitex	55,000
+	Dally [4]	CFW	2,100
▲ (with grain) ▼ (against grain)	Barabanov et al [6]	molded graphite, ρ = 1.8 g/cc	2,000 - 3,000
■	Green [2]	AUF	4,000
⬬	Cocciotti [3]	pyrographite	11,000

Leichter - Fig. 5

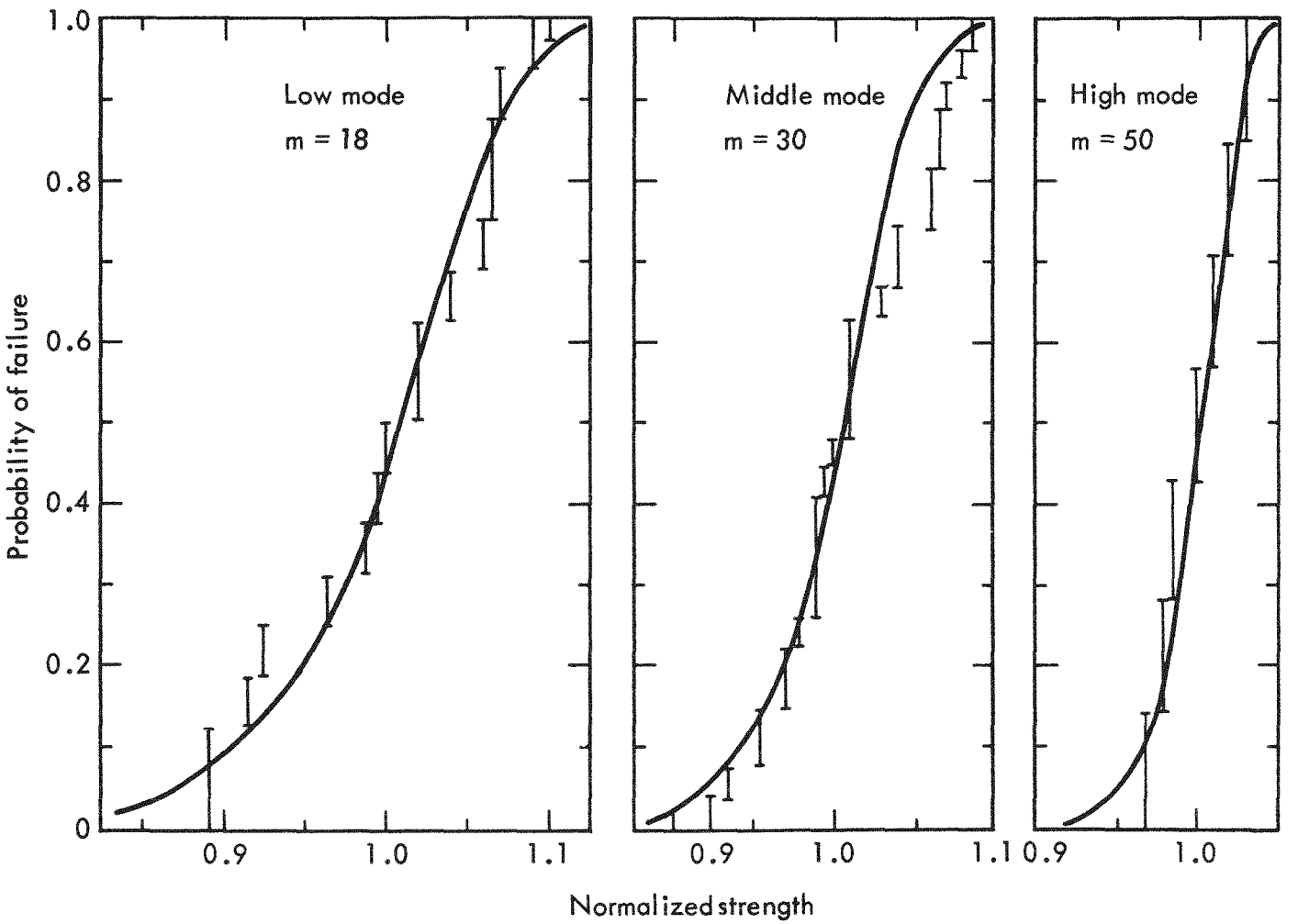

Leichter - Fig. 6

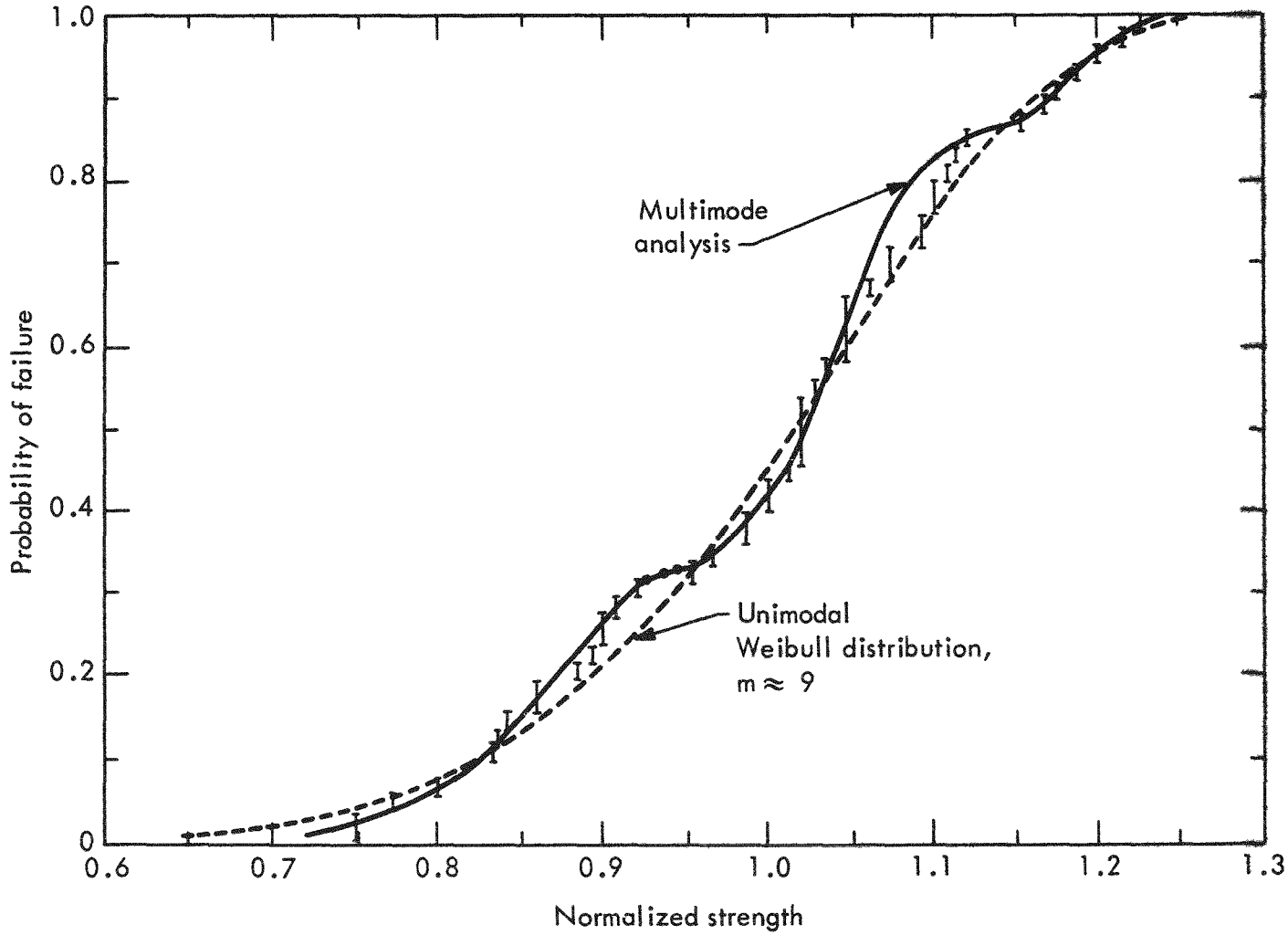

Leichter - Fig. 7

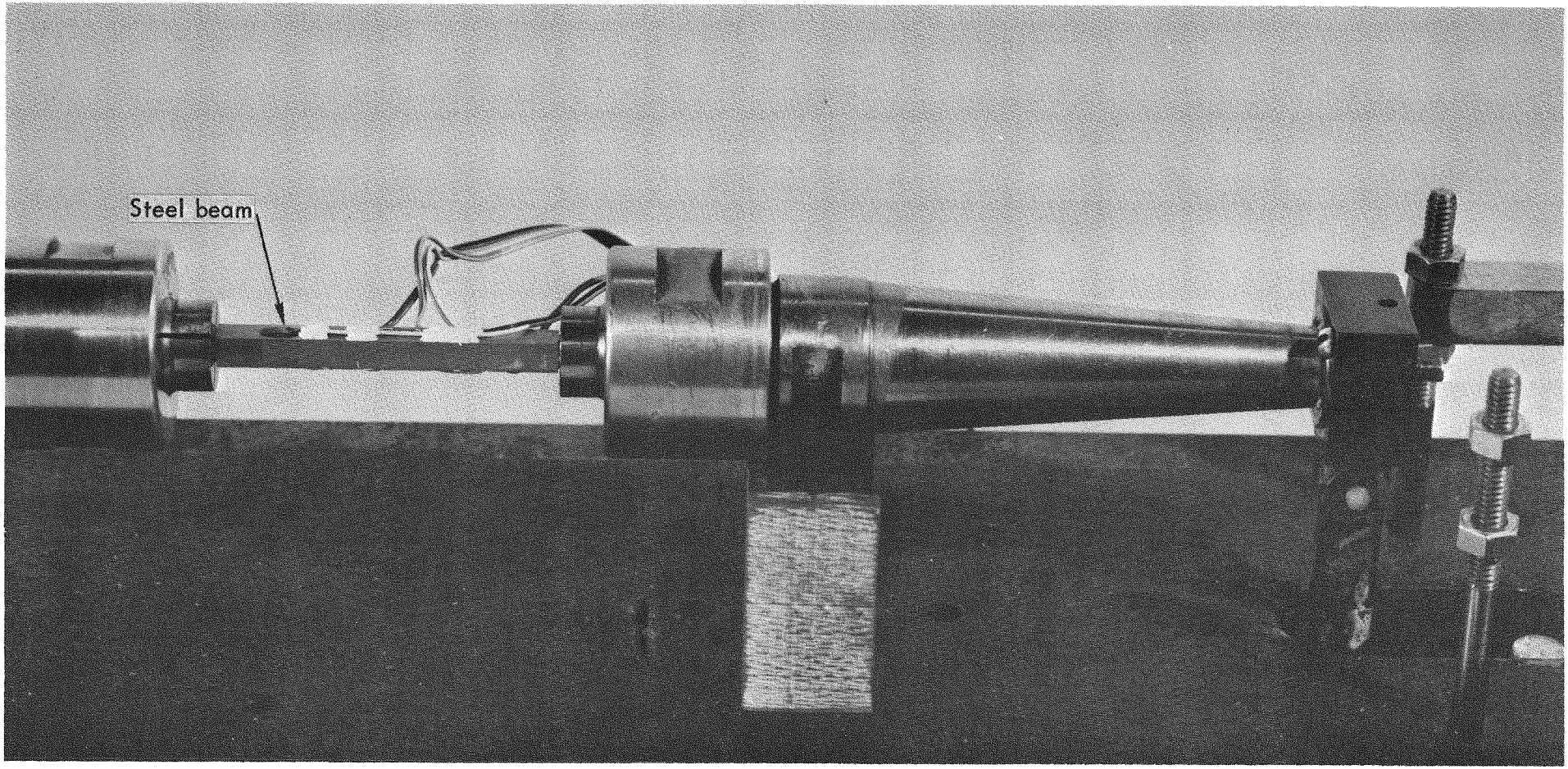

Leichter - Fig. 8

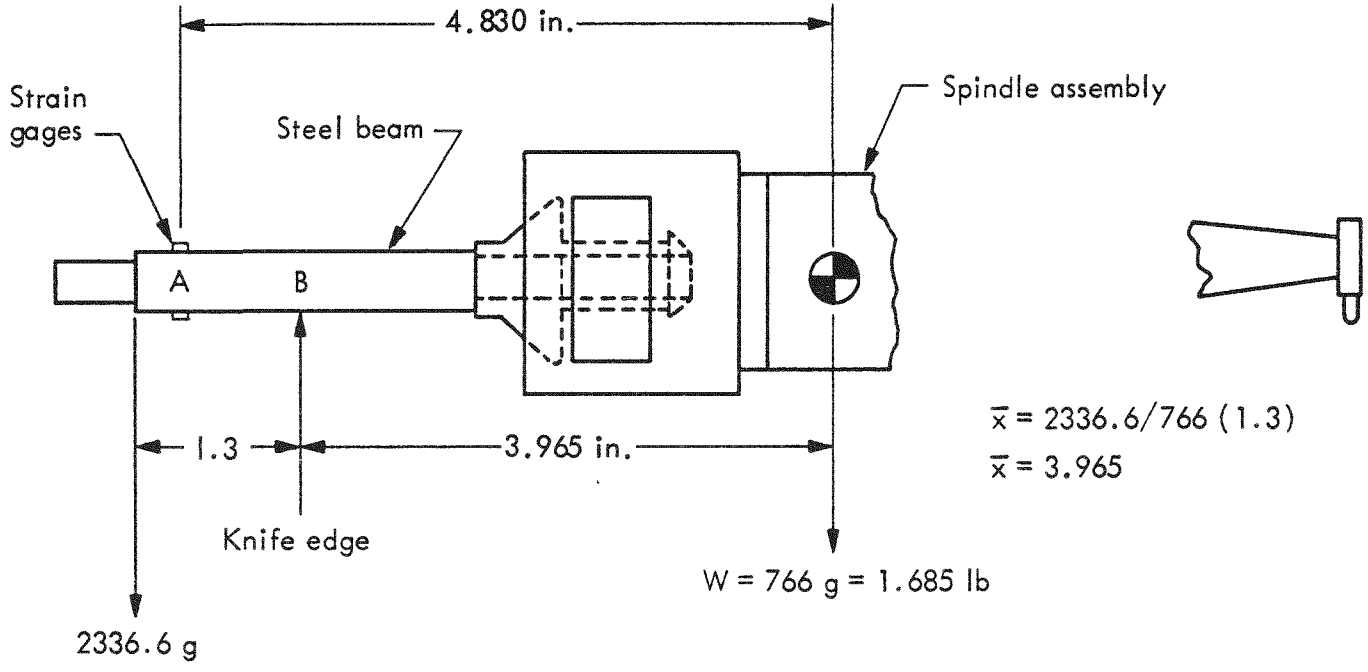

Leichter - Fig. 9

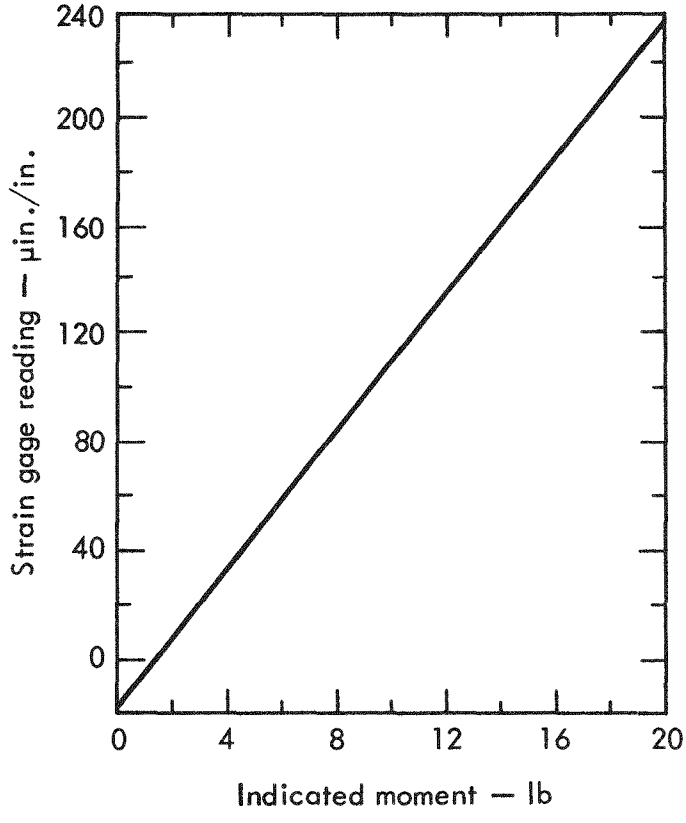

Leichter - Fig. 10

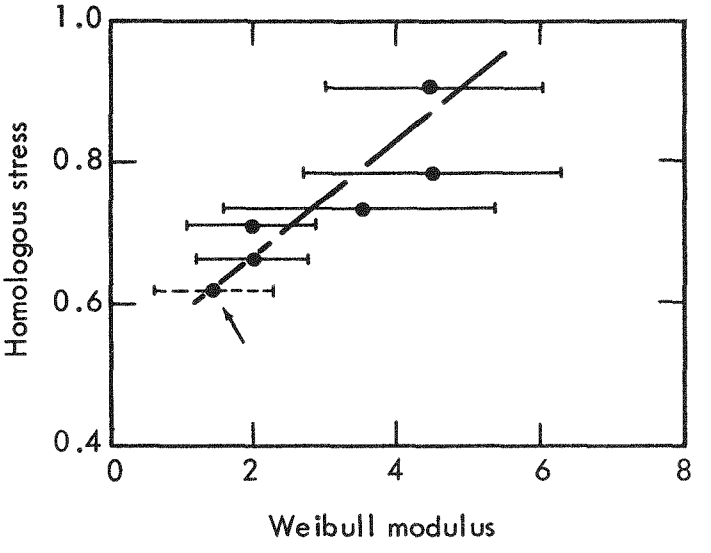

Leichter - Fig. 11

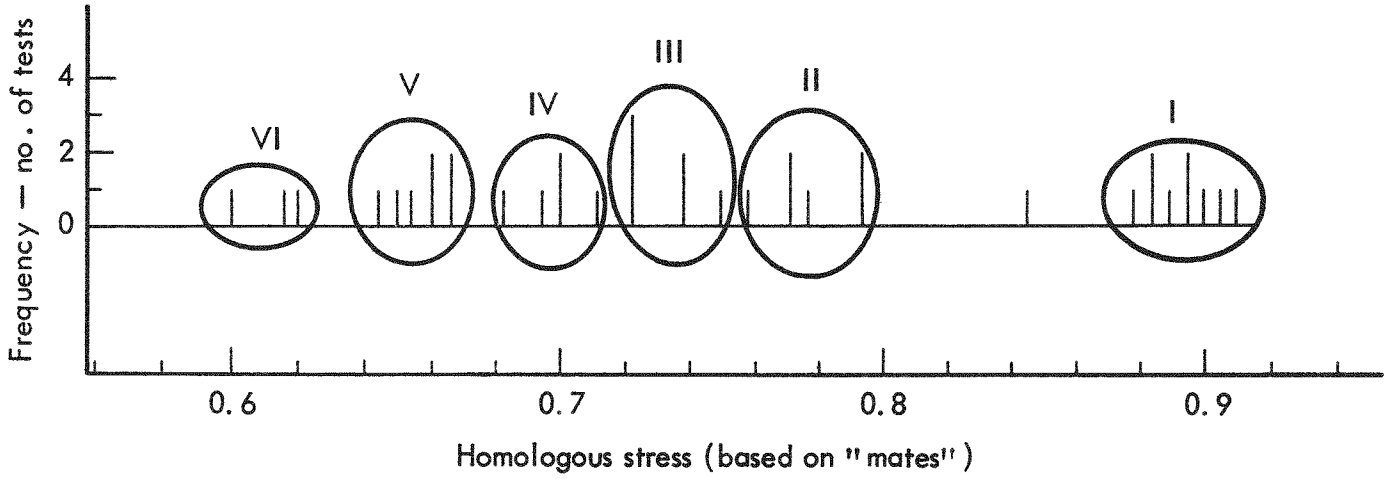

Leichter - Fig. 12

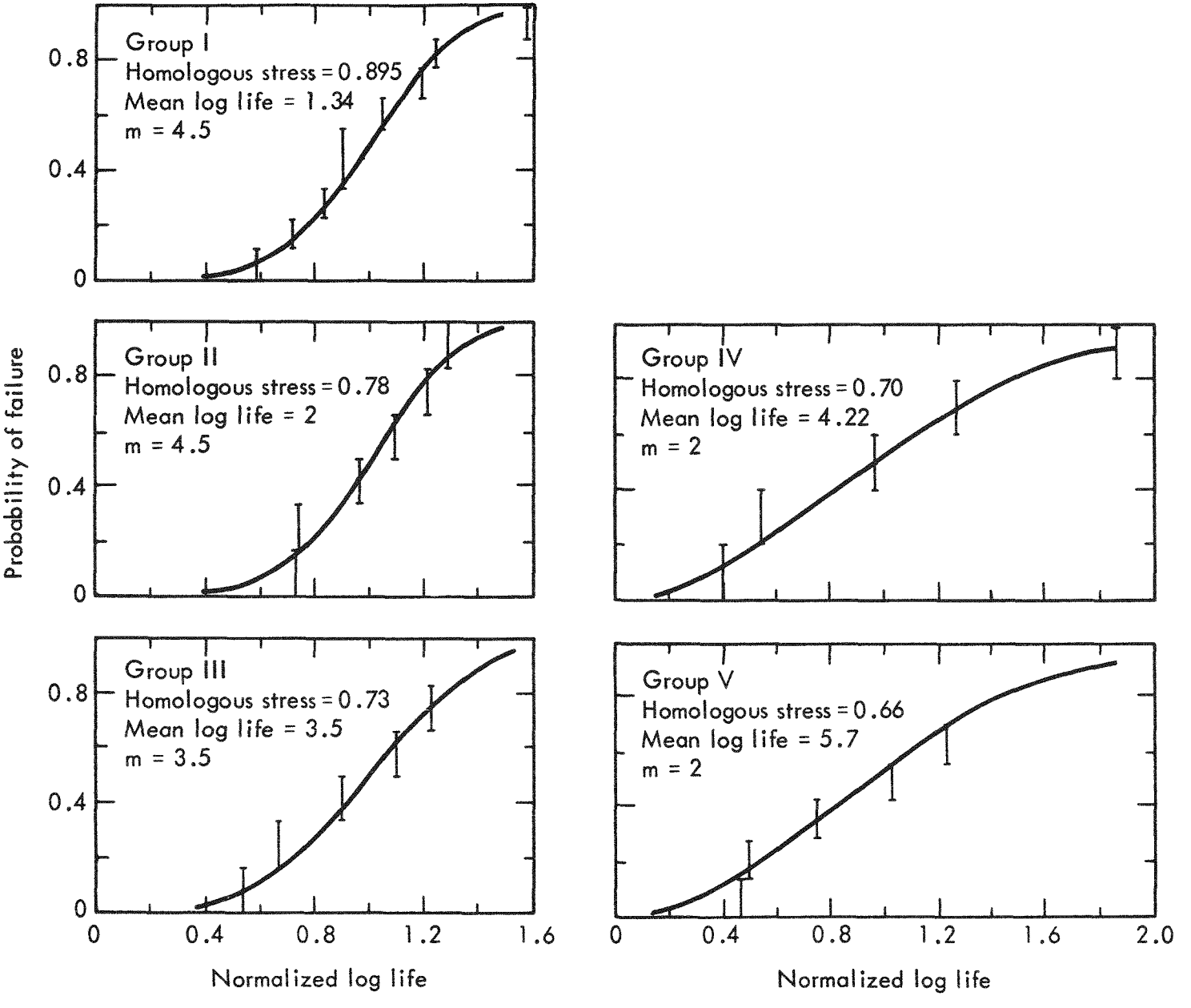

Leichter - Fig. 13

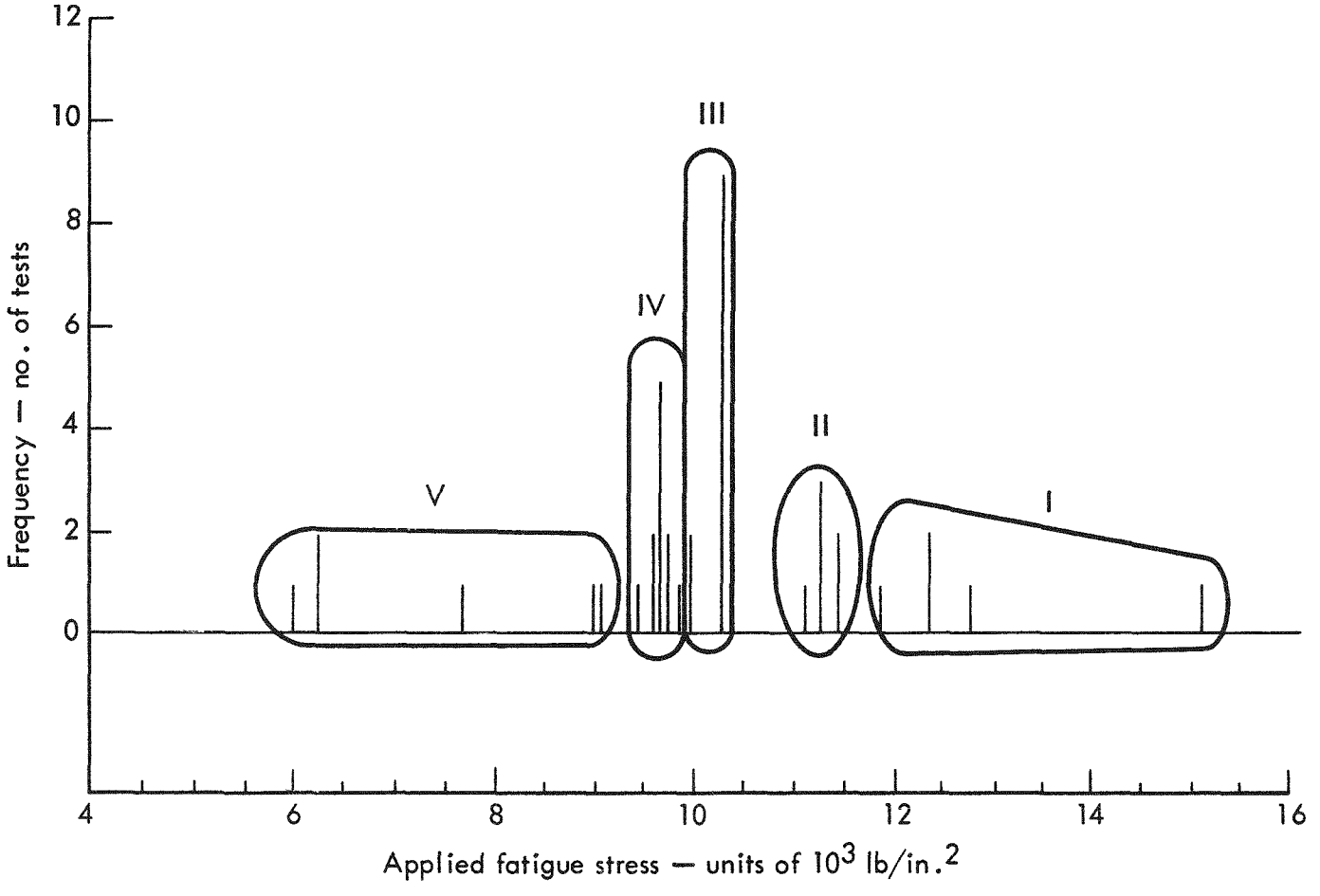

Leichter - Fig. 14

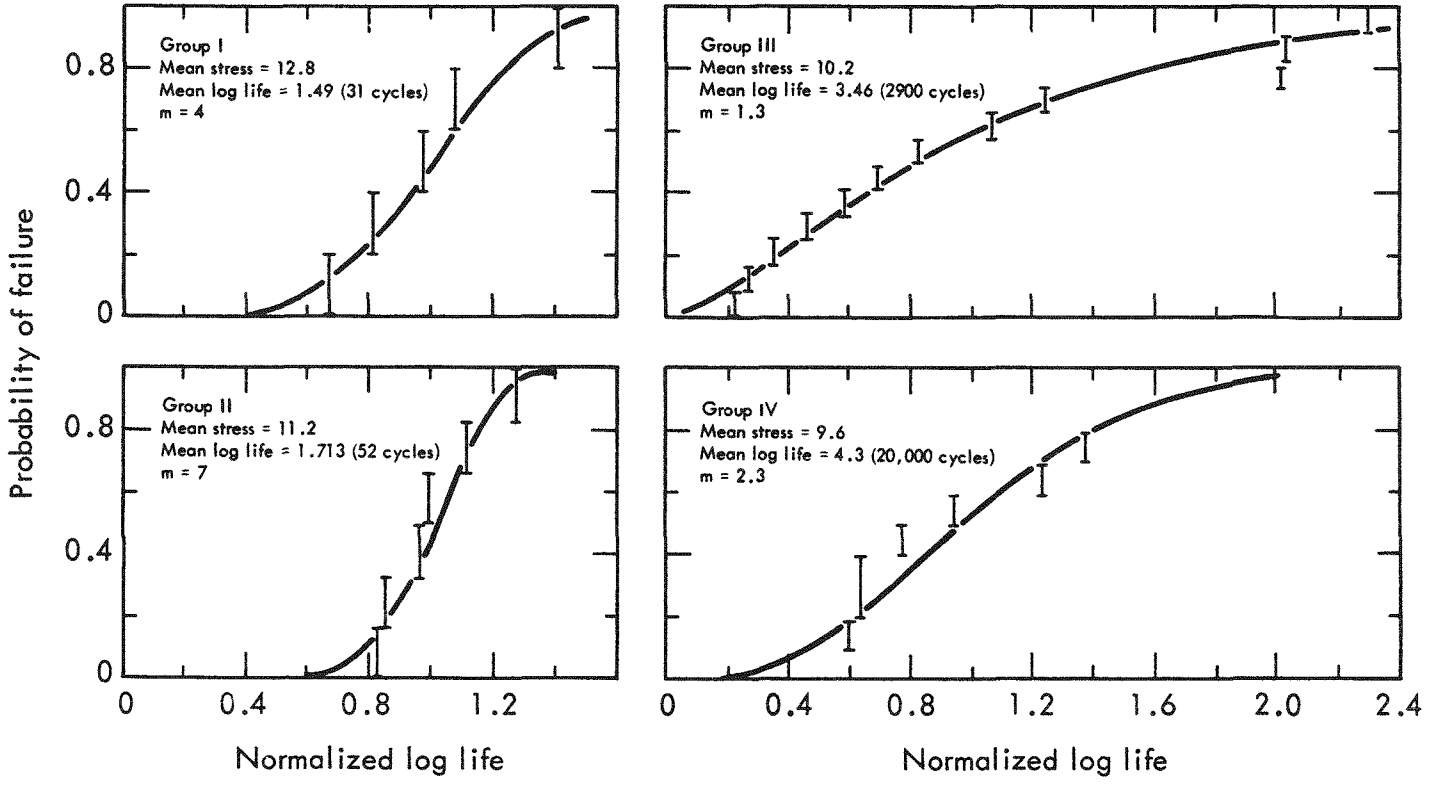

Leichter - Fig. 15

DISTRIBUTION

LRL Internal Distribution

Michael M. May

H. Leichter 6

E. Robinson 6

TID Berkeley

TID File 10

External Distribution

Division of Technical Information Extension, Oak Ridge

VRM/dh